

**An *ex vivo* model employing keloid-derived cell-seeded collagen sponges for therapy development**

Yosuke Yagi#<sup>1,2</sup>, Eri Muroga#<sup>1</sup>, Motoko Naitoh<sup>3</sup>, Zenzo Isogai<sup>4</sup>, Seiya Matsui<sup>1,5</sup>, Susumu Ikehara<sup>2</sup>, Shigehiko Suzuki<sup>3</sup>, Yoshiki Miyachi<sup>1</sup>, Atsushi Utani<sup>2</sup>

<sup>1</sup>Department of Dermatology Graduate School of Medicine, Kyoto University, Kyoto, Japan

<sup>2</sup>Department of Dermatology, Graduate School of Medicine, Nagasaki University, Nagasaki, Japan

<sup>3</sup>Plastic Reconstructive Surgery, Graduate School of Medicine, Kyoto University, Kyoto, Japan

<sup>4</sup>Department of Dermatology, National Center for Geriatrics and Gerontology

<sup>5</sup>Drug Discovery Research Laboratories, Maruho Co., Ltd., Kyoto, Japan

#These authors contributed equally to this work.

**Short title:** A glycosaminoglycan deposition model of keloids

**Corresponding author:** Atsushi Utani, MD, PhD

Department of Dermatology, Graduate School of Medicine, Nagasaki University,

1-7-1 Sakamoto, Nagasaki 852-8501, Japan

Tel: +81-95-819-7331; Fax: +81-95-849-7335

E-mail: utani@nagasaki-u.ac.jp

**Abstract**

The most distinctive feature of keloid is the extreme deposition of extracellular matrix, including collagens and proteoglycans. The focus of this study was the proteoglycan versican, which presumably defines keloid volume due to its ability to retain large amounts of water through its component glycosaminoglycans. The excessive deposition of versican in keloids was examined by immunohistochemical analysis, and up-regulation of the versican gene in these lesions by real-time PCR. The latter showed that mesenchymal cells derived from keloid lesions (KL cells) continue to exhibit above-normal versican production in culture.

To establish a model of glycosaminoglycan deposition in keloids, collagen sponges seeded with KL cells (KL-SPos) were implanted in the subcutaneous space of nude mice. After one month, the KL-SPos were significantly heavier than the Fb-seeded sponges (Fb-SPos). This *ex vivo* model was subsequently used to IL-1 $\beta$  for its ability, which was identified to reduce versican *in vitro*. Among these, IL-1 $\beta$  or chondroitinase ABC, when injected directly, successfully reduced the weight of the KL-SPos. Thus, based on the change in weight of the seeded sponges, this *ex vivo* model can be used to test therapies aimed at reducing or inhibiting keloid formation and to study the pathogenesis of this aberrant response.

## Introduction

Keloids occur spontaneously or following minor trauma, expanding beyond the boundaries of the original wound and causing serious functional and cosmetic problems. In people predisposed to keloid development, normal wound healing processes are derailed, leading to an exuberant cellular response that includes excessive extracellular matrix (ECM) production and deposition (Wolfram *et al.*, 2009).

Our group (Naitoh *et al.*, 2005) as well as others (Smith *et al.*, 2008) determined that ECMs are overexpressed in keloid tissues and cells, respectively, as determined using microarray assays. Recently, we demonstrated that micro-RNA-mediated mechanisms, namely a significant decrease in the level of miR196, was involved in the increased collagen synthesis characteristic of keloids (Kashiyama *et al.*, 2012). In addition, we showed that in these lesions, elastic fiber formation is disrupted due to the excess amounts of the glycosaminoglycan (GAG) chondroitin sulfate (CS) and dermatan sulfate (DS) (Ikeda *et al.*, 2009).

Versican is a member of the CS/DS-proteoglycan (PG) family. It is distributed in a variety of soft tissues and participates in cell adhesion, migration, proliferation, differentiation, and cartilage development (Matsumoto *et al.*, 2006; Wu *et al.*, 2005).

The sulfate or carbonyl moieties that from the long GAG side chains of versican enable it to hold large amounts of water. Since excessive PG deposition contributes significantly to keloid volume, the elimination of these molecules by targeted treatment would significantly contribute to resolving the clinical problems associated with keloid development. Currently, international clinical recommendations on scar management,

including keloids, comprise several treatment modalities (Mustoe *et al.*, 2002). However, among these, triamcinolone, surgery, radiation, and combination therapy have been shown to actually promote the recurrence of keloids rather than permanently eliminate them (Al-Attar *et al.*, 2006; Butler *et al.*, 2008; van de Kar *et al.*, 2007). The difficulty in developing a successful therapeutic strategy is further complicated by the absence of an appropriate model of keloids, a refractory disorder that is specific to humans.

The GAG deposition model of keloids developed in this study was based upon our observation of increased versican transcription in primary cultured keloid cells, as determined in promoter assays. Sponges seeded with these aberrant cells were implanted into the subcutaneous space of nude mice and used to study the inhibitory effect of several compounds. Of the cytokines and growth factors tested, only IL-1 $\beta$  inhibited versican expression. Thus, this animal model provides an invaluable approach to the development of effective therapies aimed at reducing keloid formation, which can then be tested in human trials. Furthermore, it can be used to identify the *in vivo* components that promote ECM formation in these abnormal tissues.

## **Results**

### **Versican accumulation and up-regulation of the gene in keloids**

In a previous study (Ikeda *et al.*, 2009), we found that the ECM deposited in keloids contains large amount of CS and DS. Microarray assays analyzing these tissues showed that versican and other PGs comprising the ECM were expressed at higher levels than in nonlesional skin (Naitoh *et al.*, 2005). To confirm that versican is

expressed at aberrantly high levels in keloids, we subjected six samples of keloids (K1-K6) to histopathological analysis. Hematoxylin-eosin staining revealed numerous fibrillar collagenous matrices forming a whorled pattern and a central collection of broad, compact, hyalinized, collagenous bundles (**Figure 1a**). The presence of massive amounts of GAGs in these matrices was evidenced by toluidine blue staining (**Figure 1a**). Immunohistochemical analysis with anti-versican antibody demonstrated intense versican deposition in the keloids, but not in nonlesional skin (**Figure 1a**). However, there was no difference in hyaluronan accumulation (**Figure 1a**). These observations suggest that versican is a specific marker of keloids.

Alternative splicing produces several versican isoforms, designated V0–V3 (Wu *et al.*, 2005). Two major versican transcripts, namely the V0 and V1 isoforms, were detected in both normal human skin and in keloids by RT-PCR analysis (data not shown). Real-time PCR analysis of the three keloid-derived RNAs and the three normal skin-derived RNAs revealed substantially higher versican mRNA levels in keloids than in normal skin (**Figure 1b**). Semi-quantitative RT-PCR of the six keloid-derived RNAs (K1–K6) and the RNAs derived from five normal skin samples (N1–N5), showed a similar tendency (data not shown).

### **Primary cultured cells derived from keloids continue to overexpress PGs**

Eight keloid cell lines (KL cells) were established from eight individuals and eight normal fibroblast lines (Fb) were established from another eight. Microarray analysis of the ECM using KL and Fb cell line showed that the former continued to overexpress ECM, and showed up-regulation of three PGs (versican, aggrecan, and lumican) under the culture conditions used (**Table 1**); all three PGs are up-regulated

in tissues (Naitoh *et al.*, 2005).

### **Up-regulation of versican expression in KL cells**

To determine whether versican is specifically up-regulated in primary cultured KL cells, versican mRNA levels were measured. As shown by real-time PCR, the ratio of versican to GAPDH expression in KL cells was 2.54 +/- 0.53-fold higher than that in Fb (n=5 for both KL cells and Fb) (**Figure 2a**). Furthermore, we used luciferase reporter assays to examine the activity of the versican promoter region, spanning -559 to +353, in KL cells and Fb. As shown in **Figure 2b**, luciferase activity was 1.73 +/-0.22-fold higher in KL cells. After confirming that antibody 2B1 specifically bound to versican, we performed dot blot analysis, which showed that KL cells over-produce versican protein (4.71 +/- 2.53-fold higher than Fb; **Figure 2c**).

### **Regulation of versican expression**

Hypothesizing that a decrease in versican expression would lead to a corresponding reduction in keloid volume, we screened various cytokines, growth factors, and signaling-pathway inhibitors. We carried out a series of studies in which LY294002, SB202190, and PD98059 were used to inhibit the PI3K, p38 MAPK, and ERK pathways, respectively. The results showed that PI3K and p38 MAPK, but not ERK, stimulated versican expression in both KL cells and Fb (**Figure 3a**).

Among the growth factors and cytokines tested. The addition of IL-1 $\beta$  to Fb and KL cells reduced versican expression in both, by 49.6 +/- 13% and 21.2 +/- 3.3%, respectively, compared to the corresponding untreated cells (**Figure 3b**). These results are consistent with other

studies in which IL-1 $\beta$  reportedly suppressed versican expression in gingival fibroblasts (Qwarnstrom *et al.*, 1993) and in arterial smooth muscle cells (Lemire *et al.*, 2007). Exogenous IL-1 $\beta$  also suppressed relative promoter activity in Fb and KL cells, as evidenced by a decrease in luciferase activity of 65.8 +/- 6.9% and 36.5 +/- 10%, respectively (**Figure 3c**).

We then examined whether differences in the expression of IL-1 $\beta$  and IL-1 receptors by KL cells and Fb accounted for the differential response to IL-1 $\beta$  and thus for the up-regulation of versican in KL cells. ELISA assays showed that the amounts of endogenous IL-1 $\beta$  protein in the conditioned medium of both cell types were below the detectable limit (data not shown). Furthermore, according to real-time PCR, KL cells and Fb contain similar levels of IL-1 receptor mRNA in (data not shown). Finally, the addition of an IL-1 receptor antagonist did not affect versican expression, although it completely blocked L-1 $\beta$ -induced versican down-regulation (**Figure 3d**). These results indicate that endogenous IL-1 $\beta$  is not involved in versican gene regulation, under these experimental conditions.

### **Generation of an *ex vivo* GAG deposition model in mice**

As noted above, keloid formation occurs only in humans and so there is no appropriate animal model. We therefore sought to establish an *ex vivo* model using the ECM-overproducing KL cells. In a previous study, we found that cartilage could be successfully reconstructed using a collagen sponge as a scaffold for chondroprogenitor cells (Togo *et al.*, 2006). Accordingly, these sponges, which consist of chemically cross-linked collagen resistant to collagenase digestion *in vivo*, were used in our *ex vivo* model. Collagen sponges were seeded with  $5 \times 10^5$  KL

cells (KL-SPO) or Fb (Fb-SPO) and then implanted into the subcutaneous space of nude mice (**Figure 4a**). After various incubation periods, the KL-SPO and Fb-SPO were removed and weighed. After 1 month the KL-SPOs were less translucent (**Figure 4a**) and were significantly heavier than the Fb-SPOs (29 mg  $\pm$  8.1 mg vs. 17 mg  $\pm$  6.9 mg, respectively; **Figure 4a**). In contrast, a 3-dimensional *in vitro* incubation of KL-SPOs and Fb-SPOs for 1 month did not result in significant weight differences (**Figure 4b**). In sponges incubated subcutaneously for 1 month, hematoxylin-eosin and Alcian-blue staining showed, respectively, that greater amounts of ground substances and GAGs had been deposited in the KL-SPOs than in the Fb-SPOs (**Figure 4c**). Immunostaining evidenced larger amounts of versican but not of hyaluronan (data not shown) in the KL-SPOs than in the Fb-SPOs (**Figure 4d**).

### **Injections with chondroitinase ABC or IL-1 $\beta$ reduced implant growth**

The implants were treated with chondroitinase ABC to determine whether the weight increase in the KL-SPO could be suppressed by removing the CS/DS chains of PGs, including versican. Weekly injections of 0.5 U of chondroitinase ABC for 1 month caused a significant reduction in the weight of KL-SPO (from 26 mg  $\pm$  6.7 mg to 14 mg  $\pm$  6.8 mg; **Figure 5a**). In the KL-SPOs, Alcian-blue staining revealed that the chondroitinase ABC injections had substantially reduced GAG deposition (**Figure 5b**), while versican immunostaining demonstrated that the enzymatic removal of the CS/DS chains caused significant decrease in the levels of the core proteins of the PGs (**Figure 5b**). These data suggest that versican deposition in the KL-SPOs is mediated by CS/DS-chain interactions with other matrix components. By contrast, the amount of collagen deposition in the injected KL-SPOs

and uninjected KL-SPos was essentially the same, as shown by Masson-trichrome staining (**Figure 5b**).

Since exogenous IL-1 $\beta$  reduced versican expression *in vitro*, we tested its effect on KL-SPos. Although there were no significant differences in alcian blue staining, Masson-trichrome staining, and versican immunostaining between IL-1 $\beta$  treated and non-treated sponges (data not shown), a significant reduction of weight was achieved with thrice-weekly injections of the cytokine (**Figure 5c**).

## Discussion

While it is clear that normal wound healing processes are derailed in individuals predisposed to developing keloids, the pathogenic mechanisms of keloids are poorly understood, including those resulting in excess ECM production (Wolfram *et al.*, 2009). PGs are expressed in large amounts in keloids and, because of their GAG-mediated capacity to retain large amounts of water, are likely to play important roles in determining the volume of these aberrant tissues. We previously reported that the GAGs deposited in keloid tissues mainly consist of CS/DS (Ikeda *et al.*, 2009). Of the three PGs showing increased expression in keloids, lumican GAGs only carry keratan sulfate chains. Because the major glycosaminoglycan found in keloids is chondroitin sulfate (Ikeda *et al.*, 2009), we ruled out lumican as one of the PGs whose level is increased in keloids. In our earlier study of keloids, we were unable to detect aggrecan expression by northern blotting; thus, we assumed its expressions to be weak in keloid tissue (Naitoh *et al.*, 2005). Therefore, we focused on versican as the major PG deposited in keloids.

Several groups have attempted to generate animal models of keloids (e.g., by implanting tissue piece of human keloid tissue into mice (Polo *et al.*, 1998; Waki *et al.*, 1991)), however, to date, they have not been widely used (Ramos *et al.*, 2008). Recently, hypertrophic scar tissue implanted into nude mice was shown to undergo a significant size reduction in response to the direct application of basic fibroblast growth factor (Eto *et al.*, 2011). However, we preliminarily tried to implant small pieces of keloid tissue into nude mice, but after one month these pieces had undergone various degrees of size reduction, probably due to matrix degradation. It may be that size is a critical factor in the prolonged maintenance of the implanted tissue, which is influenced by the proper distribution of nutrients and/or oxygen from the surrounding tissue. In an earlier study, we succeeded in obtaining cartilage production in the subcutaneous space of nude mice by using a chemically cross-linked collagen sponge seeded with chondroprogenitor cells (Togo *et al.*, 2006). Accordingly, we speculated that these sponges would be an excellent material for studying the mechanisms of GAG deposition in keloids. Indeed, after one month, the KL-SPos were heavier than the Fb-SPos. This result in turn implied that the efficacy of test compounds in suppressing keloid volume could be estimated simply by weighing the sponges. Another advantage of the collagen sponges is that their elasticity facilitates injection with the various candidate therapeutic compounds. A sponge-like scaffold fabricated from polylactic acid (Chung *et al.*, 2008) was also tested but it did not result in significant versican deposition (data not shown).

One of the aims of this study was to identify compounds that inhibited the growth of the KL-SPos. As TGF- $\beta$  stimulates versican expression in dermal fibroblasts under *in vitro* conditions (Kahari *et al.*, 1991), blockade of the TGF- $\beta$  signaling pathway may also be a potent candidate keloid treatment modality. Similarly, it would be interesting to

examine the effects of PI3K and p38MAPK inhibitors on GAG deposition in our *ex vivo* system. Down-regulation of versican deposition by IL-1 $\beta$  was observed in KL cells in our *ex vivo* model. Thus, IL-1 $\beta$  may be of therapeutic interest in keloids. Chondroitinase ABC may also be a potent inhibitor of keloid formation based on its ability to remove GAGs, as demonstrated in our *ex vivo* model. A reduction in keloid volume would be sufficient to relieve many of the clinical symptoms and cosmetic problems of affected individuals. Chondroitinase ABC is currently being tested in a phase III clinical trial in the USA and Japan for the treatment of interdisc herniation (<http://www.seikagaku.co.jp/english/pdf/76.pdf>). The results of that trial may be applicable to the treatment of keloids. While, there are currently several treatment modalities for keloids, many are unsatisfactory because they fail to prevent recurrence (Butler *et al.*, 2008). We developed a simple, reliable *ex vivo* model of keloids that can be used not only to evaluate novel anti-keloid agents but also to identify the mechanisms underlying the pathogenesis of keloids.

## **Materials and methods**

### **Keloid samples and primary culture**

Keloids are defined as raised, red, and inflexible scar tissue that invades the boundaries of the original wound (Butler *et al.*, 2008). Keloids and unaffected normal skin tissue specimens were obtained surgically with informed consent and the approval of the Ethical Committee of the Kyoto University Medical School. Tissue samples were taken from keloids located on the shoulder, chest, or abdomen of six individuals (K1~K6, male:female ratio=4:2; mean age=36.3), and from normal skin tissue remaining after the surgical removal of benign

tumors located on the face, buttock, abdomen, or inguinal region of five individuals (N1~N5, male:female ratio=1:4; mean age=31.6). All of the samples were subjected to histological examination and mRNA extraction.

Primary cultured cells were obtained from keloids located on the face, shoulder, chest, back, or abdomen of another eight individuals (male:female ratio=6:2; mean age=29.4), and from the normal skin of the face, forearm, buttock, or abdomen of eight additional individuals (male:female ratio=5:3; mean age=31.4). Primary cell culture involved plating small pieces of excised keloid tissue on plastic dishes in 10% FBS/DMEM with antibiotics and incubating the cultures at 37°C until cells grew out of the tissue pieces. These cells were maintained in the same culture medium and passaged by a 1:2–3 split when they reached early confluence.

For the signal inhibition assay, KL cells and Fb were cultured in medium containing 30  $\mu$ M LY294002 (PI3K inhibitor), 30  $\mu$ M SB202190 (p38 MAPK inhibitor), or 20  $\mu$ M PD98059 (ERK inhibitor; all from Calbiochem, Damstadt, Germany). For IL-1 $\beta$  signaling studies, the cells were cultured in the presence of IL-1 $\beta$  (20 U/ml; Roche Diagnostics, Indianapolis, IN). RNA was purified 15 h after IL-1 $\beta$  treatment. Recombinant IL-1 receptor antagonist (0.5  $\mu$ g/ml; R&D systems, Minneapolis, MN) was applied to both the KL cells and the Fb 24 h before RNA purification.

### **Animals and operations**

The number of animals used in this study was kept to a minimum and all possible efforts were made to reduce their suffering, in compliance with protocols established by the Animal Research Committee of Kyoto

University.

### **Immunohistochemistry**

For versican immunostaining, mouse anti-human versican monoclonal antibody (2B1; from Seikagaku Kogyo Co. Ltd. Tokyo, Japan) and Cy3-conjugated anti-mouse IgGs (Millipore-Chemicon, Billerica, MA) were used according to the manufacturer's instructions. For hyaluronan immunostaining, biotinylated-hyaluronic acid-binding protein (Seikagaku Kogyo Co. Ltd. Tokyo, Japan) and streptavidin-Cy3 (Sigma-Aldrich, St. Louis, MO) were used according to the manufacturer's instructions. Fluorescence immunostaining was analyzed by confocal laser scanning microscopy using a Zeiss LSM 510 system (Carl Zeiss Microscopy, Gottingen, Germany).

### **Real-time PCR**

Total RNA was extracted and cDNA was synthesized as previously reported (Ikeda *et al.*, 2009). RT-PCR products were analyzed by quantitative real-time RT-PCR by using TaqMan probe (Roche Applied Science, Mannheim, Germany), TaqMan Universal PCR Master Mix (Applied Biosystems, Carlsbad, CA), and the respective primers (Sigma-Aldrich, St. Louis, MO) according to the manufacturer's instructions. Triplicate reactions were performed in an AB7300 real-time thermocycler (Applied Biosystems, Carlsbad, CA) under the following thermal cycles: 2 min at 50°C, 1 min at 95°C, and 40 cycles of 15 s at 95°C and 1 min at 60°C. The TaqMan probe and primers used were as follows: GAPDH, probe #60, forward primer, (83–101 nt Genbank™ NM\_002046.3) 5'-AGCCACATCGCTCAGACAC and reverse primer (130–148 nt) 5'-GCCCAATACGACCAAATCC; versican, probe

#54, forward primer (9,657–9,675 nt Genbank™ NM\_004385.3)  
5'-GCACCTGTGTGCCAGGATA and reverse primer (9,703–9,726 nt)  
5'-CAGGGATTAGAGTGACATTCATCA; and IL-1 receptor, probe  
#60, forward primer (1,350–1,371 nt Genbank™ NM\_000877.2)  
5'-TG TTCATTTATGGAAGGGATGA and reverse primer (1,403–1,427  
nt) 5'-TTCTGCTTTTCTTTACGTTTTTCATT.

### **Transfection and luciferase assays**

The promoter activity of KL cells and Fb was assessed by inserting a -559 to +353 region of the human versican gene (GenBank™ U15963) (Naso *et al.*, 1994) upstream of the luciferase gene in the pTAL-luc plasmid (BD Biosciences Clontech, Palo Alto, CA). The construct was verified by DNA sequencing. KL cells or Fb were seeded on 24-well plates at  $1.5 \times 10^5$  cells per well and transfected with Fugene HD (Roche Applied Science, Mannheim, Germany) and measured their luciferase activities with a Promega Dual Luciferase Reporter Assay kit (Promega, Madison, WI) according to manufacturer's protocols.

### **Western and dot blot analysis of versican protein**

To collect conditioned medium,  $2.0 \times 10^5$  KL cells or Fb were seeded on 6-well plates. Two days after serum starvation induced by culture in 2 ml of DMEM, conditioned medium was collected and used for western blot and dot blot analysis, which were done as described previously (Isogai *et al.*, 1996; Koyama *et al.*, 2007). Intensities of dots were calculated using ImageQuant TL (GE Healthcare, Amersham Place, England). The values were expressed as the ratios to cell numbers.

### **Generation of an *ex vivo* GAG deposition model**

Collagen sponges were prepared and were implanted into subcutaneous pockets of nude mice as previously reported (Togo *et al.*, 2006). Before implanting sponges, they were incubated overnight in 10% FBS/DMEM with  $5 \times 10^5$  KL cells or Fb, thus generating KL-SPo and Fb-SPo, respectively. Four weeks after implantation, the KL-SPo and Fb-SPo were removed, weighed, and subjected to histological analysis as follows: after fixation with 10% phosphate-buffered formalin for 24 h at 4°C, the sponges were embedded in paraffin and sliced into 7.0  $\mu\text{m}$  sections, which were either stained with hematoxylin-eosin or Alcian-blue (pH 2.5), or subjected to immunohistochemical analysis.

### **Injection of the collagen sponges with chondroitinase ABC and IL-1 $\beta$**

KL-SPOs were injected once a week, starting 1 week post-implantation, with *Proteus vulgaris* chondroitinase ABC (protease free: 0.1 units in 50  $\mu\text{l}$  of 0.1% BSA/H<sub>2</sub>O) or IL-1 $\beta$  (40 units in 20  $\mu\text{l}$  of 0.1% BSA/PBS). An equal amount of vehicle served as the control. At 4 weeks post-implantation, the mice were killed and the sponges removed and analyzed.

### **cDNA microarray analysis**

Total RNA was isolated from cultured KL cells and Fb using an RNeasy mini kit (Qiagen, Valencia, CA). Total RNA (1  $\mu\text{g}$ ) was amplified and labeled using the One-Cycle Target Labeling kit (Affymetrix, Santa Clara, CA).

Biotin-labeled cRNA (15 $\mu\text{g}$ ) was fragmented and hybridized to the GeneChip Human Genome U133 Plus 2.0 Array (Affymetrix). The array

was incubated and signals were scanned according to the manufacturer's protocol. Expression profiles were analyzed based on the MAS5 algorithm using GeneChip operating software (Affymetrix), with further analysis using GeneSpring 7.3 (Agilent Technologies, Palo Alto, CA). Raw intensity values from each chip were normalized to the 50th percentile of the measurements. Each gene was normalized to the median of that gene in the respective controls to enable comparison of relative changes in gene expression levels between different conditions.

### **Statistical analysis**

Student's t test was used to examine differences between experimental groups. The data are expressed as the means +/- standard deviation (S.D.). The calculated *p* values were two-sided; *p* < 0.05 was considered statistically significant.

**Conflict of interest:** none.

### **Acknowledgments**

We thank Dr. Yoshihiko Yamada and Dr. Kenneth Yamada, National Institute of Dental and Craniofacial Research, National Institutes of Health, for critical reading of the manuscript and helpful suggestions. This work was supported in part by Grants-in-Aid (nos. 20591344, 23659511) for Scientific Research from the Ministry of Education, Culture, Sports, Science and Technology of Japan, and by a grant from the Nakatomi Foundation to A.U.

## References

- Al-Attar A, Mess S, Thomassen JM, Kauffman CL, Davison SP (2006) Keloid pathogenesis and treatment. *Plast Reconstr Surg* 117:286-300.
- Butler PD, Longaker MT, Yang GP (2008) Current progress in keloid research and treatment. *J Am Coll Surg* 206:731-41.
- Chung HJ, Steplewski A, Chung KY, Uitto J, Fertala A (2008) Collagen fibril formation. A new target to limit fibrosis. *J Biol Chem* 283:25879-86.
- Eto H, Suga H, Aoi N, Kato H, Doi K, Kuno S, et al. (2011) Therapeutic potential of fibroblast growth factor-2 for hypertrophic scars: upregulation of MMP-1 and HGF expression. *Lab Invest* advance online publication, 26 September 2011; doi:10.1038/labinvest.2011.127.
- Ikeda M, Naitoh M, Kubota H, Ishiko T, Yoshikawa K, Yamawaki S, et al. (2009) Elastic fiber assembly is disrupted by excessive accumulation of chondroitin sulfate in the human dermal fibrotic disease, keloid. *Biochem Biophys Res Commun* 390:1221-8.
- Isogai Z, Shinomura T, Yamakawa N, Takeuchi J, Tsuji T, Heinegard D, et al. (1996) 2B1 antigen characteristically expressed on extracellular matrices of human malignant tumors is a large chondroitin sulfate proteoglycan, PG-M/versican. *Cancer Res* 56:3902-8.
- Kahari VM, Larjava H, Uitto J (1991) Differential regulation of extracellular matrix proteoglycan (PG) gene expression. Transforming growth factor-beta 1 up-regulates biglycan (PGI), and versican (large fibroblast PG) but down-regulates decorin (PGII) mRNA levels in human fibroblasts in culture. *J Biol Chem* 266:10608-15.

Kashiyama K, Mitsutake N, Matsuse M, Ogi T, Saenko VA, Ujifuku K, et al. (2012) miR-196a Downregulation Increases the Expression of Type I and III Collagens in Keloid Fibroblasts. *J Invest Dermatol*.

Koyama H, Hibi T, Isogai Z, Yoneda M, Fujimori M, Amano J, et al. (2007) Hyperproduction of hyaluronan in neu-induced mammary tumor accelerates angiogenesis through stromal cell recruitment: possible involvement of versican/PG-M. *Am J Pathol* 170:1086-99.

Lemire JM, Chan CK, Bressler S, Miller J, LeBaron RG, Wight TN (2007) Interleukin-1beta selectively decreases the synthesis of versican by arterial smooth muscle cells. *J Cell Biochem* 101:753-66.

Matsumoto K, Kamiya N, Suwan K, Atsumi F, Shimizu K, Shinomura T, et al. (2006) Identification and characterization of versican/PG-M aggregates in cartilage. *J Biol Chem* 281:18257-63.

Mustoe TA, Cooter RD, Gold MH, Hobbs FD, Ramelet AA, Shakespeare PG, et al. (2002) International clinical recommendations on scar management. *Plast Reconstr Surg* 110:560-71.

Naitoh M, Kubota H, Ikeda M, Tanaka T, Shirane H, Suzuki S, et al. (2005) Gene expression in human keloids is altered from dermal to chondrocytic and osteogenic lineage. *Genes Cells* 10:1081-91.

Naso MF, Zimmermann DR, Iozzo RV (1994) Characterization of the complete genomic structure of the human versican gene and functional analysis of its promoter. *J Biol Chem* 269:32999-3008.

Polo M, Kim YJ, Kucukcelebi A, Hayward PG, Ko F, Robson MC (1998) An in vivo model of human proliferative scar. *J Surg Res* 74:187-95.

Qwarnstrom EE, Jarvelainen HT, Kinsella MG, Ostberg CO, Sandell LJ, Page RC, et al. (1993) Interleukin-1 beta regulation of fibroblast proteoglycan synthesis involves a decrease in versican steady-state mRNA levels. *Biochem J* 294 ( Pt 2):613-20.

Ramos ML, Gragnani A, Ferreira LM (2008) Is there an ideal animal model to study hypertrophic scarring? *J Burn Care Res* 29:363-8.

Smith JC, Boone BE, Opalenik SR, Williams SM, Russell SB (2008) Gene profiling of keloid fibroblasts shows altered expression in multiple fibrosis-associated pathways. *J Invest Dermatol* 128:1298-310.

Togo T, Utani A, Naitoh M, Ohta M, Tsuji Y, Morikawa N, et al. (2006) Identification of cartilage progenitor cells in the adult ear perichondrium: utilization for cartilage reconstruction. *Lab Invest* 86:445-57.

van de Kar AL, Kreulen M, van Zuijlen PP, Oldenburger F (2007) The results of surgical excision and adjuvant irradiation for therapy-resistant keloids: a prospective clinical outcome study. *Plast Reconstr Surg* 119:2248-54.

Waki EY, Crumley RL, Jakowatz JG (1991) Effects of pharmacologic agents on human keloids implanted in athymic mice. A pilot study. *Arch Otolaryngol Head Neck Surg* 117:1177-81.

Wolfram D, Tzankov A, Pulzl P, Piza-Katzer H (2009) Hypertrophic scars and keloids—a review of their pathophysiology, risk factors, and therapeutic management. *Dermatol Surg* 35:171-81.

Wu YJ, La Pierre DP, Wu J, Yee AJ, Yang BB (2005) The interaction of versican with its binding partners. *Cell Res* 15:483-94.

## Figure legends

### Figure 1

Versican accumulation and up-regulation in keloids.

- a) Hematoxylin-eosin (HE) staining revealed the deposition of an abnormal fibrillar collagenous matrix within the keloids. Toluidine blue (TB) staining at pH 2.5 showed metachromasia, indicative of GAG accumulation in the keloids. Arrows point to the boundary of the lesion. The keloids contained large deposits of versican but there was no increase in hyaluronan (HA) levels. Representative images of the keloids obtained from six individuals are shown. Bar, 100  $\mu$ m.
- b) Real-time PCR analysis of versican mRNA expression in samples of normal skin and of keloids. Mean  $\pm$  SD and versican/GAPDH ratios are shown.

### Figure 2

Versican up-regulation in cultured KL cells. a) KL cells and Fb were analyzed for versican expression by real-time PCR. Versican/GAPDH ratios were calculated by setting the versican mRNA expression of one Fb cell line at 100%. The mean  $\pm$  SD and the versican/GAPDH ratios are shown. b) Both cells were transfected with a versican promoter luciferase reporter construct containing the versican promoter region (-559 ~ +353) and part of exon 1 fused to the luciferase gene. Luciferase activity was measured in quadruplicate and was calculated by setting the luciferase activity of one Fb cell line at 100%. Shown are the mean

luciferase activities  $\pm$  S.D. c) The antibody 2B1 specifically bound to versican (around 450 kDa). Dot blot analysis of versican protein in conditioned medium.

### Figure 3

Analysis of signaling pathways and the effects of IL-1 $\beta$  on versican expression *in vitro*. a) In KL cells (closed column) and Fb (blank column), PI3K was blocked by the addition of LY294002 (LY), p38 MAPK by SB202190 (SB), and ERK by PD98059 (PD). \* $p < 0.001$ . b) KL cells or Fb were treated with IL-1 $\beta$ . c) Transfection was carried out 48 h prior to stimulation of the cells with IL-1 $\beta$  (20U/ml). d) Both cell types were treated with recombinant IL-1 receptor antagonist and/or IL-1 $\beta$ . Versican/GAPDH ratios or luciferase promoter activity were calculated by setting the value obtained from the untreated KL cells or Fb at 100%. All experiments were performed in triplicate. Representative data, expressed as the means  $\pm$  S.D., are shown.

### Figure 4

Generation of an *ex vivo* GAG deposition model in nude mice. a) KL-SPo or Fb-SPo was implanted into the subcutaneous space of the mice (upper two images). After 1 month, the sponges were removed (lower two images). The mean  $\pm$  S.D. of the increase in the weights of the sponges are shown. b) Collagen sponges seeded or not with KL cells or Fb were cultured. The mean  $\pm$  S.D. of the weights of samples are shown. c) Sponges were stained with HE (hematoxylin-eosin), AB (Alcian-blue), and nuclear fast red. The arrowhead indicates the chemically cross-linked collagen fibers of the collagen sponges, and the arrow the ground substance deposits. Bar, 1 mm or 50  $\mu$ m. d) Versican

immunostaining of KL-SPos and Fb-SPos. Bar, 100  $\mu$ m.

**Figure 5**

IL-1 $\beta$  injections reduce implant growth. a) KL-SPos were transplanted into the subcutaneous space of nude mice. Chondroitinase ABC was injected into the sponges once a week for 1 month starting one week post-implantation. The sponges were then removed and immediately weighed. Shown are the mean  $\pm$  S.D. implant weights of three animals per group (-): vehicle (0.1% BSA/H<sub>2</sub>O). b) Staining with Alcian-blue (AB) or Masson-trichrome (MT), and immunostaining with anti-versican antibody of the chondroitinase ABC-treated (+) and untreated (-) KL-SPos. Bar, 50 or 100  $\mu$ m. c) IL-1 $\beta$  was injected into the sponges once or thrice a week for 1 month starting one week post-implantation. Thrice-weekly injections significantly reduced the KL-SPos weight increase.

Figure 1

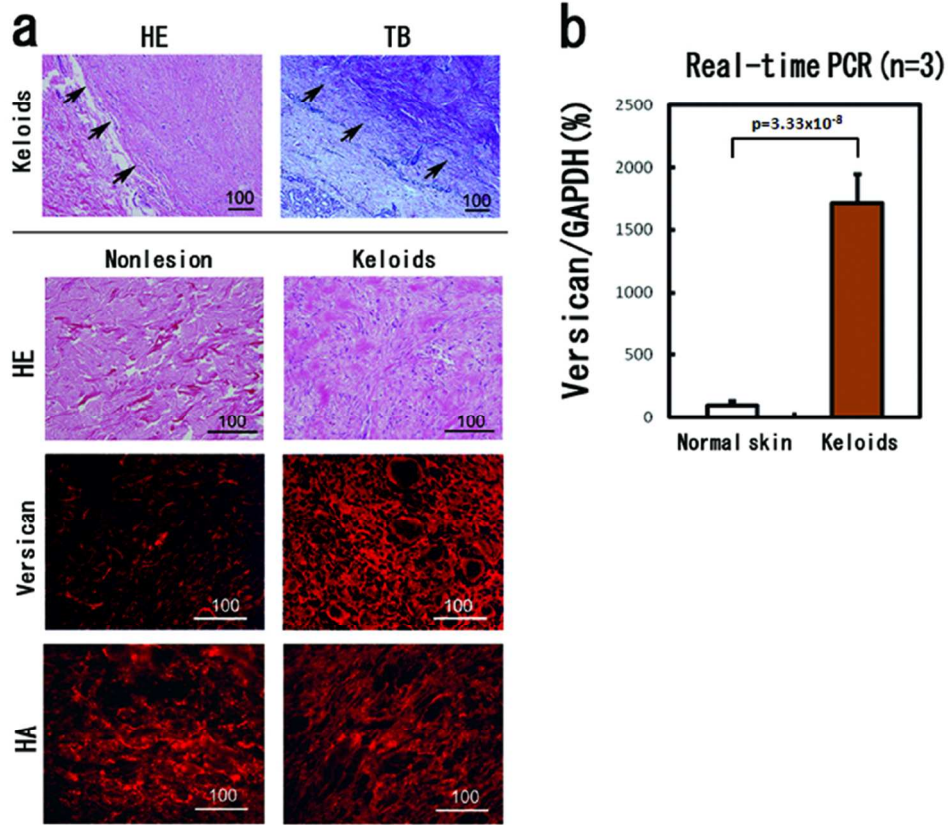


Figure 2

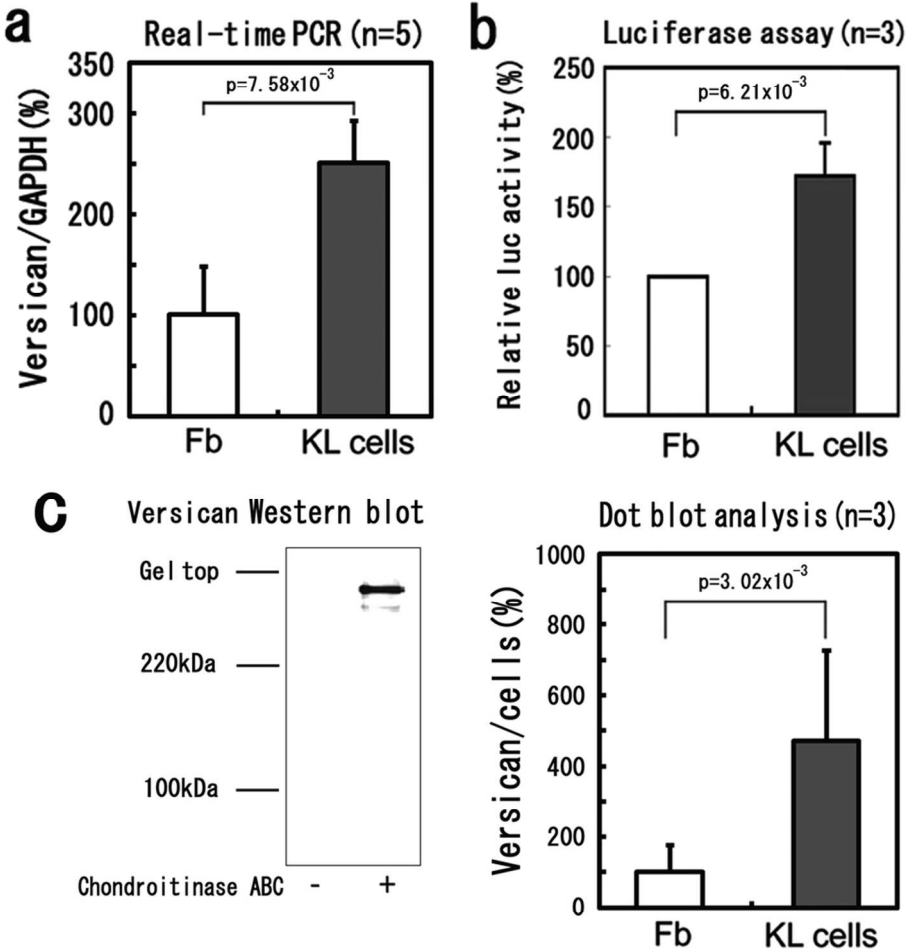


Figure 3

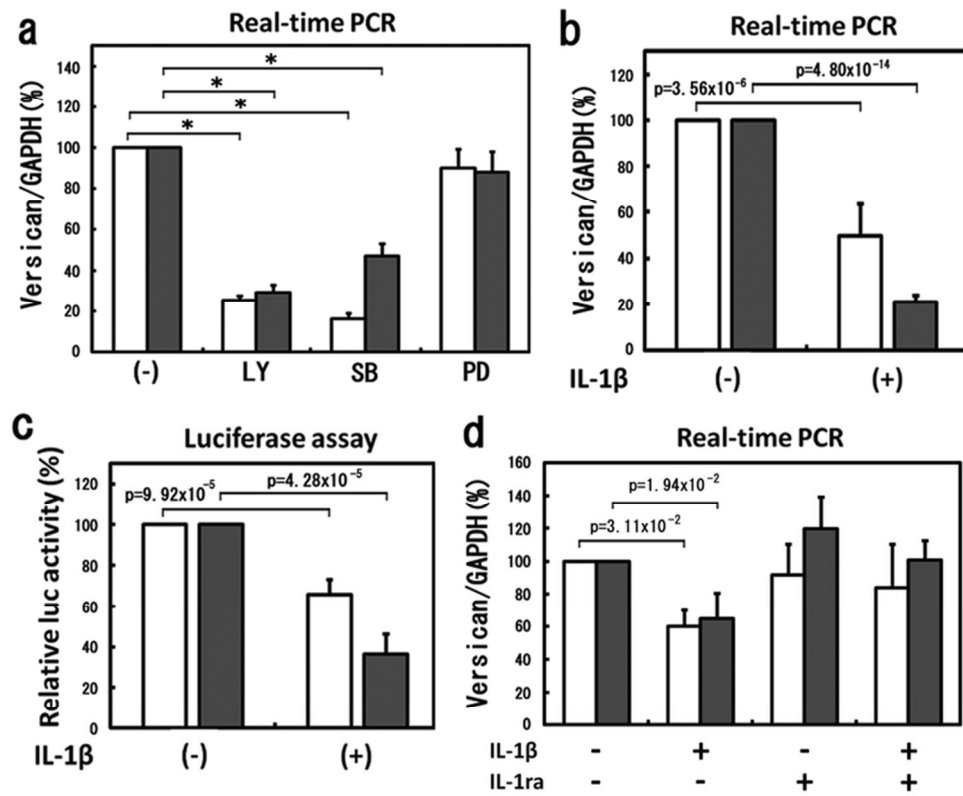


Figure 4

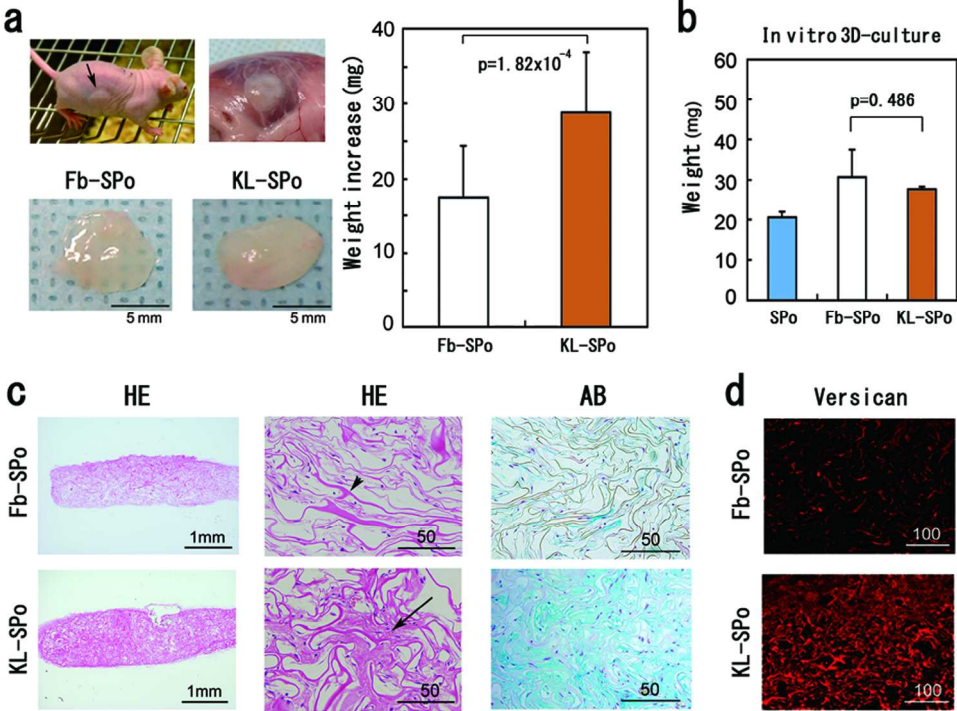
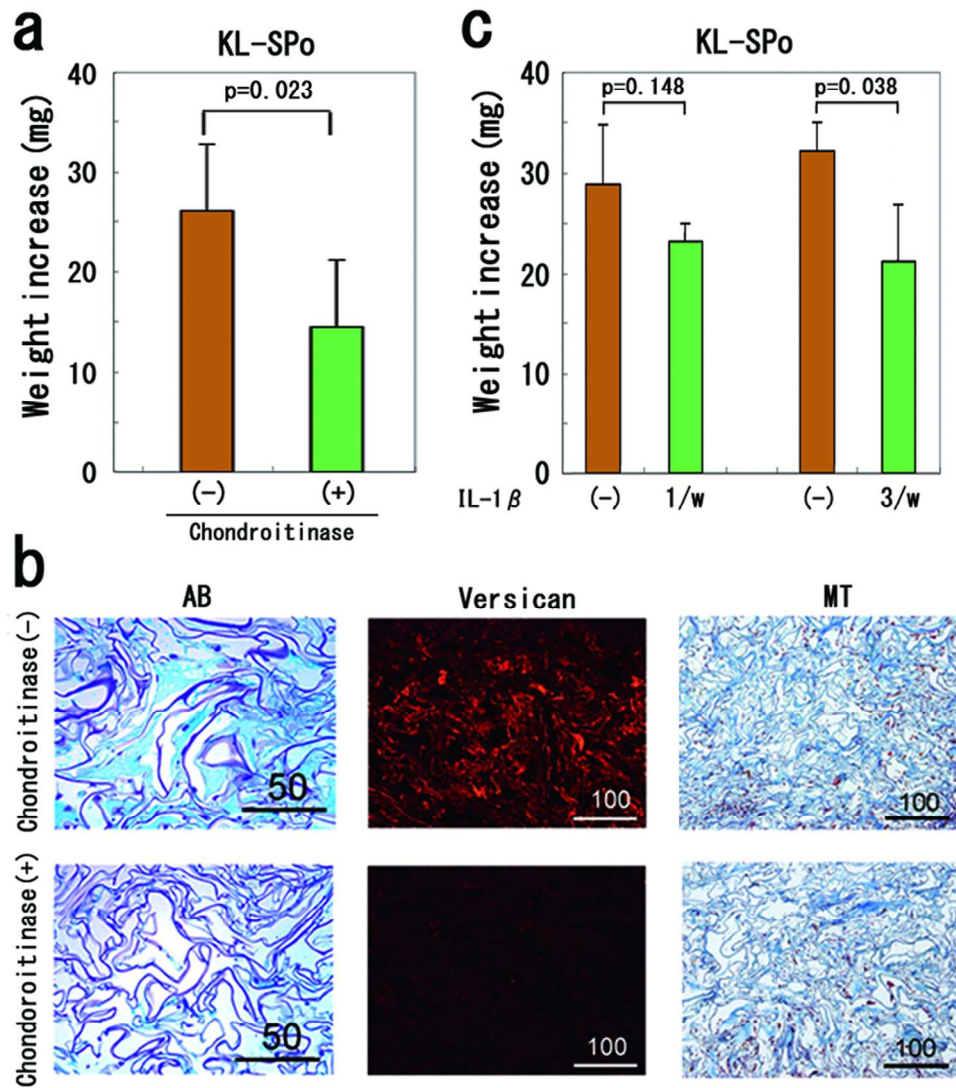


Figure 5



**Table 1. Microarray analysis of upregulated ECM genes in KL cells**

Gene	Protein	mRNA KL cells /mRNA Fb <sup>1</sup>
COL10A1	collagen $\alpha$ 1(X)	10.4
COL2A1	collagen $\alpha$ 1(II)	10.3
ACAN	aggrecan	6.2
COL9A1	collagen $\alpha$ 2(IX)	3.9
COL11A1	collagen $\alpha$ 1(XI)	3.6
LUM	lumican	3.4
COL8A1	collagen $\alpha$ 1(VIII)	2.8
VCAN	versican	2.5
THBS1	thrombospondin 1	2.4
COL17A1	collagen $\alpha$ 1(XVII)	2.2
COL9A3	collagen $\alpha$ 3(IX)	2.1

<sup>1</sup>Determined by microarray analysis performed in the current study